ChemComm

Accepted Manuscript

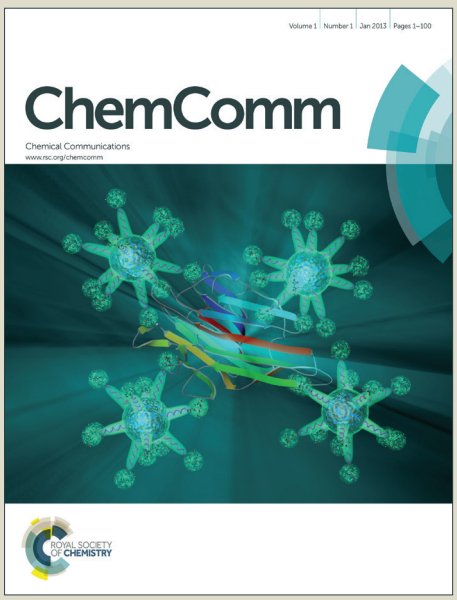

ROYAL SOCIETY OF CHEMISTRY

www.rsc.org/chemcomm

Journal Name

RSCPublishing

COMMUNICATION

Increased photocurrent in a tandem dye-sensitized solar cell by modifications in push-pull dye-design.

Cite this: DOI: 10.1039/xoxxoooooox

C. J. Wood,[a] G. H. Summers[a,b] and E. A. Gibson[a,b]*

Received ooth January 2012,
Accepted ooth January 2012

DOI: 10.1039/xoxxoooooox

www.rsc.org/

Donor-π-acceptor photosensitizers for NiO photocathodes that exhibit a broad spectral response across the visible region are presented. These enabled an increase in the photocurrent density of p-type dye-sensitized solar cells to 8.2 mA cm^{-2} and a tandem cell to be assembled which generated a photocurrent density of 5.15 mA cm^{-2}.

Dye-sensitized solar cells (DSCs) based on mesoporous semiconductor electrodes are often presented as low-cost alternatives to conventional silicon devices.[1] However to date their efficiency has only reached 13% compared to 25% for crystalline silicon.[2] State-of-the-art DSCs are based on photoanodes, so the photocurrent generated when light is absorbed is a result of electron transfer from the excited dye to the conduction band of the TiO_2, an n-type semiconductor. An efficient dye-sensitized photocathode would enable tandem cells to be constructed, where the platinised counter electrode found in n-DSCs is replaced with a dye-sensitized p-type semiconductor.[3,4] This enables more light to be converted more efficiently, giving a maximum theoretical efficiency of 43% compared to 33% for a single junction device. Despite this potential for a step-change in the photoconversion efficiency of dye-sensitized solar cells, a tandem device that is more efficient than TiO_2 alone has not been reported because an efficient p-DSC has not yet been produced. An increasing amount of work has been devoted to developing p-DSCs, where light absorption by the dye is followed by rapid electron transfer from the valence band of the semiconductor, typically NiO, to the dye.[3] However, the efficiency of p-DSCs, often based on dye-sensitized NiO, remains far lower (1.4%[5]) than that obtained for n-DSCs and so tandem devices generally have a lower efficiency[8] than typical n-type devices. This effect is further enhanced because of the overlap of the light absorption between the n- and p-type dyes.[4]

Dyes typically used in conventional TiO_2-based DSCs convert photons up to 600 nm with high quantum efficiency.[1] Therefore, dyes used for the photocathode should harvest wavelengths longer than 600 nm. To date there have been very few reports of dyes for photocathodes that absorb at longer wavelengths and generate sufficient photocurrents to be used in tandem DSCs.[6,7] Noticeably, compared to the number of recent publications on p-DSCs, relatively few tandem DSCs have been reported.[3,4]

The aim of this work was to build on our previous success with dyes incorporating a cationic 1-hexyl-2,3,3-3H-indolium acceptor unit and bodipy chromophores.[6,8] Appending these groups through a thiophene π-linker to the 4-(diphenyl amino) benzoic acid anchor/donor motif gives dyes which absorb longer wavelengths that complement state-of-the-art photoanodes in tandem cells (Figure 1). For the photoanode dye we selected D35 (Figure S1 in the ESI), a well-known push-pull sensitizer for TiO_2 that is designed to transfer electron density towards the n-type semiconductor via the carboxylic acid anchoring group.[9] Conversely, P1 pulls electrons away from the semiconductor surface and is one of the best performing dyes with NiO (reported IPCE = 63%).[10] However, the spectral response for P1 overlaps almost entirely with D35 (Figure 1). Qin *et al.* modified P1 to absorb longer wavelengths by incorporating additional cyano groups on the malonitrile acceptor unit.[10] This resulted in a significant lowering of the LUMO energy which diminished the driving force for dye regeneration[‡] by the I_3^-/I^- redox mediator such that there was a complete loss of photocurrent. The cationic 1-hexyl-2,3,3-3H-indolium acceptor dye (CAD3) was synthesised by condensing 1-hexyl-2,3,3-trimethyl-3H-indolium PF_6 onto 4-carboxy-4',4''-diformyl-2-thienyl)triphenylamine in the presence of piperidine (see ESI). The bodipy analogue (GS1) was prepared by reacting 2-phenyl-1H-pyrrole with 4-carboxy-4',4''-diformyl-2-thienyl)triphenylamine in the presence of CF_3CO_2H before oxidation with chloranil and coordination using $BF_3.O(C_2H_5)_2$.

The ground state geometry and electronic distribution in GS1 and CAD3 were predicted using hybrid-DFT calculations (See ESI). The HOMO–LUMO transition was confirmed to be the dominant electronic transition in both dyes by TDDFT (Figure S11). B3LYP is known to underestimate the energy of photoexcitation for charge transfer transitions, however the calculated solution phase spectra compare well with the experimental data presented in Figure S11.[11] The isodensity plots illustrate the "push-pull" nature of the dyes by predicting that this low energy transition is accompanied by a shift of electron density from the 4-(diphenyl amino) benzoic acid anchor/donor unit (HOMO) to the bodipy (LUMO) in GS1 or 1-hexyl-2,3,3-trimethyl-3H-indolium (LUMO) for CAD3. The optical and electrochemical properties of CAD3 and GS1 determined experimentally are summarised in the ESI (Table S1). CAD3 has a very broad absorption spectrum with λ_{max} well towards the red (Figure S3 and S4). Adsorption of CAD3 onto NiO gave rise to a 48 nm hypsochromic shift indicating strong electronic interaction between the dye and the NiO. When GS1 was adsorbed on NiO there

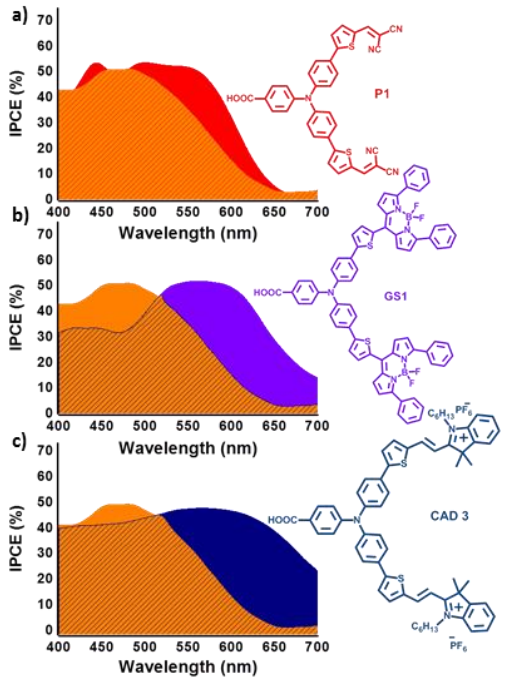

Figure 1. Overlaid IPCE plots for a **P1** (a), **GS1** (b), **CAD 3** (c) NiO p-DSC and a D35 TiO_2 n-DSC (orange) with the molecular structures adjacent. The structure of D35 is provided in Figure S1 in the ESI.

Table 1. Photovoltaic Performance of p-DSCs and Tandem p/n DSCs.

Dye	Cell type	J_{SC} [mA cm^{-2}][a)]	V_{OC} [mV]	*FF* [%]	η [%]	IPCE [%][b)]	Dye Loading [10^{-6} mol cm^{-2}][c)]
CAD3	p-DSC	8.21	101	31	0.25	50	7.36×10^{-06}
	p/n-DSC	5.15	613	54	1.7		
GS1	p-DSC	5.87	106	31	0.20	53	1.04×10^{-05}
	p/n-DSC	4.54	638	43	1.3		
P1	p-DSC	5.37	89	33	0.16	54	1.24×10^{-05}
	p/n-DSC	3.71	732	38	1.1		

[a)] *Jsc* is the short-circuit current density at the $V = 0$ intercept, *Voc* is the open-circuit voltage at the $J = 0$ intercept, *FF* is the device fill factor, η is the power conversion efficiency; [b)] ICPE is the monochromatic incident photon-to-current conversion efficiency; [c)] number of moles of dye absorbed on a 0.2 cm^2 area NiO electrode.

was no shift in the peak maximum but a broadening of the absorption spectra was observed. The molar absorption coefficient was lower for GS1 (at λ_{max}= 565 nm, ε = 66 000 L mol^{-1} cm^{-1}) than for CAD3 (at λ_{max}= 614 nm, ε = 95 000 L mol^{-1} cm^{-1}) but higher than P1.[10] GS1 and CAD3 were only mildly emissive in chlorinated solvents but luminesced sufficiently for us to estimate the lowest electronic transition energy (E_{0-0} = 1.78 eV for CAD3 and E_{0-0} = 2.11 eV for GS1) from the intercept of the normalised absorption and emission spectra. The electrochemical properties of CAD3 and GS1 were investigated by cyclic voltammetry and differential pulse voltammetry, the results are provided in the ESI. GS1 is more easily reduced than CAD3 and the first reduction process was reversible for GS1 but not for CAD3.

For the p-DSC to work, the energy levels of the dye must be carefully positioned so that there is a spontaneous "downhill" process for the electron transfer from the NiO valence band to the dye HOMO and from the dye LUMO to the redox electrolyte. The main challenge associated with dyes that absorb at longer wavelengths is that the frontier orbitals must be brought closer in energy but the orbital energy dictates the estimated driving force for charge separation (ΔG_{inj}) and dye regeneration (ΔG_{reg}).[‡] According to Liu *et al.* $\Delta G_{inj} > -0.8$ eV is required for efficient photoinduced charge separation at the dye/NiO interface.[12] We estimate[‡] ΔG_{inj}(CAD3) ≈ –0.91 eV and ΔG_{inj} (GS1) ≈ – 0.98 eV, this implies that these new dye molecules should be able to withdraw electrons from NiO following light absorption. Charge-recombination at the dye/semiconductor interface is rapid in NiO DSCs, so ΔG_{reg} of the dye by the electrolyte must be substantial in order for charge transfer in the forwards direction to compete with the reverse process.[10] We estimate[‡] ΔG_{reg} (CAD3) ≈ –0.17 eV and ΔG_{reg} (GS1) ≈ –0.54 eV indicating that electron density on either the indolium or bodipy moiety can be intercepted by the redox electrolyte.[13] Less energy is wasted in these electron transfer processes for CAD3 and GS1 than for P1(ΔG_{inj} (P1) ≈–1.21 eV and ΔG_{reg} (P1) ≈–0.64 eV).

An n-DSC incorporating D35 and three p-DSCs incorporating P1, GS1 and CAD3 were assembled using platinised conductive glass counter electrodes and infiltrated with I_3^-/I^- electrolyte. Figure 1 shows the spectral response of the p-DSCs compared to the n-DSC and Table 1 lists the p-DSC characteristics. Shifting the λ_{max} of the dyes to longer wavelength means more photons are absorbed leading to a higher photocurrent density from the p-DSC. Of the three dyes, the CAD3 device had the highest spectral response in the red region and had the highest efficiency.

The photocurrent density obtained with GS1 was almost twice that generated with the previous bodipy dye reported by our group, which was based on 2,4-dimethyl-3-ethylpyrrole.[8] By avoiding methyl substituents at the 2 position of the bodipy, the electron delocalisation has been extended from the triphenylamine-thiophene donor motif to the bodipy in GS1, as evidenced by the isodensity plots in Figure S12. Accordingly, the HOMO-LUMO gap has been reduced, broadening and red-shifting the absorption by the dye from λ_{max} = 540 nm previously to λ_{max} = 565 nm for GS1. This change in structure and optical properties has had a direct impact on the p-DSC characteristics, increasing the IPCE from 28% previously to 53% for GS1. Extending the spectral response to the red for CAD3 led to a photocurrent density of 8.2 mA cm^{-2}. This is more than double the photocurrent density we previously obtained using asymmetric indolium cationic electron-acceptor dyes (CAD1: J_{SC} = 3.6 IPCE = 33% and CAD2: J_{SC} = 3.3 mA cm^{-2} IPCE = 27%).[6] The high molar absorption coefficient of CAD3 is almost four times that of CAD1 and CAD2 and we attribute the improvement in photocurrent to the increased light harvesting efficiency of the CAD3 electrode.[6]

Recently two papers have reported improved photocurrent densities for p-DSCs using push-pull dyes; Click *et al.* obtained 7.4 mA cm^{-2} by incorporating two perylene units per dye molecule ("BH4"), giving a molar absorption coefficient of 100 000 L mol^{-1} cm^{-1},[14] Liu *et al.* achieved 7.57 mA cm^{-2} by substituting thiophene units for fluorene units, extending the π-linker ("zzx-op1–2").[14] However, the spectral response only extends to 650 nm and therefore if this dye was incorporated in a tandem cell, both electrodes would be competing for light. Our modifications to the push-pull design by substituting the electron acceptor to capture more of the solar spectrum has led to an even higher photocurrent density. The IPCE for each dye was *c.a.* 50%, which is impressive for NiO p-DSCs, but lower than reported for P1 (63%), PMI-6T-TPA (62%) and zzx-op1–2 (74%).[4,10,15] Since ΔG_{inj} is sufficient for charge separation, we attribute the lower IPCEs recorded in this work to inefficient dye-regeneration by I_3^- and/or differences in the NiO preparation compared to other groups. This gives us confidence that even higher photocurrent densities are possible, providing that the frontier orbital energies of the dyes and the quality of the NiO are further optimised. The V_{OC} for the cells containing CAD3 (101 mV) and GS1 (106 mV) were slightly better than those obtained with P1 (89 mV) and only

slightly lower than that reported for zzx-op1−2 (117 mV).[10,15] Inspection of the dark current curves (Figure S15) suggests that the recombination reaction between the NiO and the electrolyte is accelerated for P1, causing the slightly lower photovoltage. The low fill factors are typical for p-DSCs and are due to a combination of detrimental dark and light induced recombination reactions.[16]

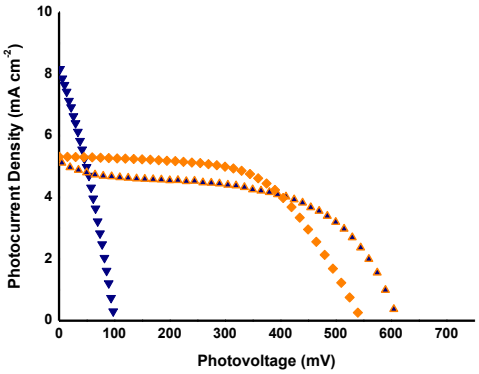

Figure 2. Current-voltage plots for a CAD3/NiO p-DSC (triangles), D35/TiO_2 n-DSC (diamonds) and a D35/CAD3 p/n DSC (open triangles).

The promising photocurrents, and unprecedented current response in the red region, prompted us to assemble p/n tandem DSCs with P1, GS1 and CAD3. To achieve current matching between the photoanode and photocathode, the film thickness of the TiO_2 electrode was varied and current-voltage and IPCE measurements were taken until a current was obtained that matched the current that would be produced by the photocathode when positioned at the bottom of the cell (e.g. 5 mA cm^{-2} for a tandem DSC with CAD3, Figure S18-S20). This was challenging to achieve for P1 due to the spectral overlap with D35 which led to very low photocurrents. Very thin TiO_2 layers were used which led to good V_{OC} but the devices suffered from poor fill factors because we were unable to match the currents at the two photoelectrodes. Much better results were achieved with GS1 and CAD3 since the spectral response is red-shifted relative to P1 and D35. The current-voltage plots for the n-DSC, p-DSC and tandem DSC for CAD3 are provided in Figure 2 (the equivalent plots for GS1 and P1 are provided in Figure S21 in the ESI). The photocurrents for the CAD3/D35 and GS1/D35 cells are the highest reported so far for tandem DSCs. However, the V_{OC} for each cell, although greater than the V_{OC} of the individual n-DSC and p-DSC, was lower than typically achieved in the best n-DSCs (typically >700 mV).[1] This is a direct result of the electrolyte chosen for the devices. A high concentration of lithium ions shifts the valence band edge of the NiO to lower energy, increasing the V_{OC} in p-DSCs, but also lowers the conduction band edge of the TiO_2 lowering the V_{OC} of the n-DSC.[17,18] Attempts to use electrolyte mixtures optimised for n-DSCs resulted in very poor performances of the p-DSCs; the electrolyte that worked best in our p-DSCs caused a large drop in photovoltage at the photoanode (V_{OC} = 500-550 mV in our n-DSCs compared to 780 mV reported by Jiang *et al.*).[9] The best tandem cells were obtained with the electrolyte optimised for p-DSCs (0.1 M I_2, 1.0 M LiI).

Conclusions

By re-designing simple donor-π-acceptor dyes to capture the lower energy portion of visible light and promote photoinduced electron transfer from NiO to a I_3^-/I^- electrolyte we have increased the photocurrent density in p-DSCs from 5.4 to 8.2 mA cm^{-2}. This has enabled us to assemble tandem cells with up to 5.2 mA cm^{-2}, which is substantially higher than any previous tandem DSC. Further modifications in dye-design will enable us to increase the photocurrent even further, and alternative redox electrolytes should enable better photovoltage to be obtained. However, we believe that the main barrier to providing the promised "step-change" in solar cell efficiency is the use of NiO as the p-type semiconductor, and efforts need to be focused on discovering a semiconductor with an energetically lower lying valence band. This would allow us to exploit the dyes reported here in a tandem cell so that a V_{OC} of up to 1.5 V is achievable.

EAG thanks the Royal Society for a Dorothy Hodgkin Fellowship and Research Project and the University of Nottingham for funding.

Notes and references

[a] School of Inorganic Chemistry, The University of Nottingham, University Park, Nottingham, NG7 2PL, United Kingdom.
[b] Now at the School of Chemistry, Newcastle University, Newcastle upon Tyne, NE1 7RU, United Kingdom. E-mail: Elizabeth.gibson@ncl.ac.uk

§Nattestad *et al.* reported p/n DSC with η=1.91%, J_{SC} = 2.4 mA cm^{-2}, V_{OC} = 1079 mV, *FF* = 74% when illuminated through the TiO_2; η=2.42% when illuminated through the NiO[9])

‡ $\Delta G_{inj} = e[E_{VB}(NiO) - E_{D*/D^-}]$; $\Delta G_{reg} = e[E(I_3^-/I_2^{\bullet-}) - E_{D/D^-}]$; $E_{(D*/D)^-} = E_{(D/D-)} + E_{0\text{-}0}$; E_{VB} (NiO) ≈ –0.12 V *vs.* $Fe(Cp)_2^{+/0}$ [15]; $E^{\circ\prime}(I_3^-/I_2^{\bullet-})$ = –0.82 V *vs.* $Fe(Cp)_2^{+/0}$ in acetonitrile.[13]

Electronic Supplementary Information (ESI) available: experimental section, absorption and emission spectra, DFT calculations, electrochemistry data, solar cell characterisation. See DOI: 10.1039/c000000x/

1 A. Hagfeldt, G. Boschloo, L. Sun, L. Kloo, H. Pettersson, *Chem. Rev.* 2010, **110**,6595.
2 M. A. Green, K. Emery, Y. Hishikawa, W. Warta, E. D. Dunlop, *Prog. Photovolt.* 2014, **22**, 701.S. Mathew, A. Yella, P. Gao, R. Humphry-Baker, B. F. E. Curchod, N. Ashari-Astani, I. Tavernelli, U. Rothlisberger, M. K. Nazeeruddin, M. Grätzel, *Nat. Chem.* 2014, **6**, 242.
3 J. He, H. Lindström, A. Hagfeldt, S.-E. Lindquist, *Sol. Energy Mater. Sol.* Cells 2000, **62**, 265; F. Odobel, Y. Pellegrin, E. A. Gibson, A. Hagfeldt, A. L. Smeigh, L. Hammarström, *Coord. Chem. Rev.* 2012, **256**, 2414.
4 A. Nattestad, A. J. Mozer, M. K. R. Fischer, Y.-B. Cheng, A. Mishra, P. Bäuerle, U. Bach, *Nat. Mater.* 2010, **9**, 31.
5 S. Powar, T. Daeneke, M. T. Ma, D. Fu, N. W. Duffy, G. Götz, M. Weidelener, A. Mishra, P. Bäuerle, L. Spiccia, U. Bach, *Angew. Chem.* 2013, **52**, 602.
6 C. J. Wood, M. Cheng, C. A. Clark, R. Horvath, I. P. Clark, M. L. Hamilton, M. Towrie, M. W. George, L. Sun, X. Yang, E. A. Gibson, *J. Phys. Chem. C* 2014, **118**, 16536.
7 C.-H. Chang, Y.-C. Chen, C.-Y. Hsu, H.-H. Chou, J. T. Lin, Org. Lett. 2012, 14, 4726.
8 J.-F. Lefebvre, X.-Z. Sun, J. A. Calladine, M. W. George, E. A. Gibson, *Chem. Commun.* 2014, **50**, 5258.
9 X. Jiang, T. Marinado, E. Gabrielsson, D. P. Hagberg, L. Sun, A. Hagfeldt, *J. Phys. Chem. C*, 2010, **114**, 2799. M. Liang, J. Chen. Chem. Soc. Rev., 2013,**42**, 3453
10 P. Qin, J. Wiberg, E. A. Gibson, M. Linder, L. Li, T. Brinck, A. Hagfeldt, B. Albinsson, L. Sun, *J. Phys. Chem. C* 2010, **114**, 4738.
11 A. Dreuw, M. Head-Gordon, *Chem. Rev.* 2005, **105**, 4009.
12 Z. Liu, D. Xiong, X. Xu, Q. Arooj, H. Wang, L. Yin, W. Li, H. Wu, Z. Zhao, W. Chen, M. Wang, F. Wang, Y.-B. Cheng, H. He, *ACS Appl. Mater. Interfaces* 2014, **6**, 3448.
13 E. A. Gibson, L. Le Pleux, J. Fortage, Y. Pellegrin, E. Blart, F. Odobel, A. Hagfeldt, G. Boschloo, *Langmuir* 2012, **28**, 6485.
14 K. A. Click, D. R. Beauchamp, B. R. Garrett, Z. Huang, C. M. Hadad, Y. Wu, *Phys. Chem. Chem. Phys.* 2014, **16**, 26103.
15 Z. Liu, W. Li, S. Topa, X. Xu, X. Zeng, Z. Zhao, M. Wang, W. Chen, F. Wang, Y.-B. Cheng, H. He, *ACS Appl. Mater. Interfaces* 2014, **6**, 10614.
16 D. Dini, Y. Halpin, J. G. Vos, E. A. Gibson, (2015*). Coord. Chem. Rev.*, 2015, in press CCR-D-14-0.
17 H. Zhu, A. Hagfeldt, G. Boschloo, *J. Phys. Chem. C* 2007, **111**, 17455.
18 Y. Liu, A. Hagfeldt, X. Xiao, S. Lindquist, *Sol. Energy Mater. Sol. Cells* 1998, **55**, 267.